Geological Quarterly, 2005, **49** (2): 205–222

Palaeoenvironmental interpretation of dinosaur- and mammal-bearing continental Maastrichtian deposits, Haţeg basin, Romania

Ana-Voica BOJAR, Dan GRIGORESCU, Franz OTTNER and Zoltan CSIKI

Bojar A.-V., Grigorescu D., Ottner F. and Csiki Z. (2005) — Palaeoenvironmental interpretation of dinosaur- and mammal-bearing continental Maastrichtian deposits, Haţeg basin, Romania. Geol. Quart., **49** (2): 205–222. Warszawa

The Haţeg basin, South Carpathians, Romania, contains a thick sequence of Maastrichtian continental deposits from which a rich dinosaur and mammal fauna is known. Field data as well as mineralogical and stable isotope analyses from three representative profiles were integrated in order to reconstruct environmental conditions during Maastrichtian time. Tuştea quarry is characterized by the presence of well drained calcisols, with smectite (montmorillonite) as the main clay component. Along the profile, the $\delta^{18}O$ and $\delta^{13}C$ isotopic compositions of calcretes show a small variation, of up to 0.9‰. The profile along the Bărbat Valley shows preponderantly calcisols, the main clay mineral being smectite, with subordinate illite and chlorite. The oxygen isotopic compositions of calcretes are ~0.5‰ lighter than those from Tuştea. The soils are interpreted as having formed under more humid conditions and they are similar to those situated at the bottom of the sequence developed along Sibişel Valley. The abundant smectite from the Tuştea and Bărbat Valley deposits, as well the presence of good developed soils, reflects palaeoenvironmental conditions predominantly controlled by climate. Preliminary magnetostratigraphic data along the Sibişel Valley section indicate that sedimentation started at the end of chron C32n. All other palaeomagnetic sites distributed upstream, as far as the upper limit of this formation, have only reversed polarity and the corresponding time interval is probably chron C31r. Along this valley, the sequence shows a general coarsening upward trend. The palaeosol type changes from calcisol- to vertisol-dominated sequences. The soils are moderate to weakly developed. The mineralogical composition of the clay fraction also changes, from smectite- to illite and chlorite-dominated. These features points towards unstable tectonic conditions and higher uplift rates of the surrounding area within chron C31r. Towards the top of the sequence, the oxygen and carbon isotopic composition of calcretes become 1 and ~2‰ lighter, respectively. These changes indicate a transition from generally semi-arid towards more humid and possible cooler conditions and correlate with the worldwide trend for chron 31r.

Ana-Voica Bojar, Institute of Earth Science, Geology and Paleontology, Karl-Franzens University, A-8010 Graz, Austria, e-mail: ana-voica.bojar@uni-graz.at; Dan Grigorescu, Zoltan Csiki, Department of Geology and Geophysics, Bucharest University, Bd. Bălcescu 1, R-010041 Bucharest, Romania; Franz Ottner, Institute for Applied Geology, Peter Jordan Strasse 70, A-1190 Wien, Austria; *(received: December 3, 2004; accepted: April 15, 2005).*

Key words: Haţeg basin, Maastrichtian, dinosaur, palaeosols, stable isotopes, clay mineralogy.

INTRODUCTION

In the Haţeg basin, South Carpathians, research activity on the Late Cretaceous faunal assemblages has already a long and interesting history. In 1895, Ilona, the sister of Baron Franz Von Nopcsa, brought her brother some bones discovered by peasants working in their neighbourhoods. The baron undertook studies on the material, and published several papers concerning the deposits and their dinosaur, pterosaur, turtle, and crocodilian assemblage (Nopcsa, 1900, 1902, 1914, 1915, 1923, 1926).

After a long gap, systematic research was again restarted in the 1980's. In the course of these studies, the lithostratigraphy and chronostratigraphy of the deposits have been updated (Antonescu *et al*., 1983; Grigorescu, 1983; Grigorescu *et al*., 1990*a*; Grigorescu and Melinte, 2001; Grigorescu and Csiki, 2002). During this period, small theropods (carnivorous dinosaurs) were discovered; meanwhile the number of taxa has increased to 5 species (Grigorescu, 1984; Weishampel *et al*., 1996; Csiki and Grigorescu, 1998). Since the discovery of the first mammals in the Haţeg basin (Grigorescu, 1984), the number of species belonging to the Multituberculate order has grown continuously (Grigorescu *et al*., 1985, 1999; Radulescu and Samson, 1986; Grigorescu and Hahn, 1987; Csiki and Grigorescu, 2000). As is only seen rarely in Europe, dinosaur clutches, representing the original nests, were found with remains of hatchings of the hadrosaur *Telmatosaurus transsylvanicus* (Grigorescu *et al*., 1990*b*; Grigorescu, 1993; Weishampel *et al*., 1993). A giant pterosaur, *Hatzegopteryx thambema*, one of the largest flying creatures in the world, was discovered in the region (Buffetaut *et*

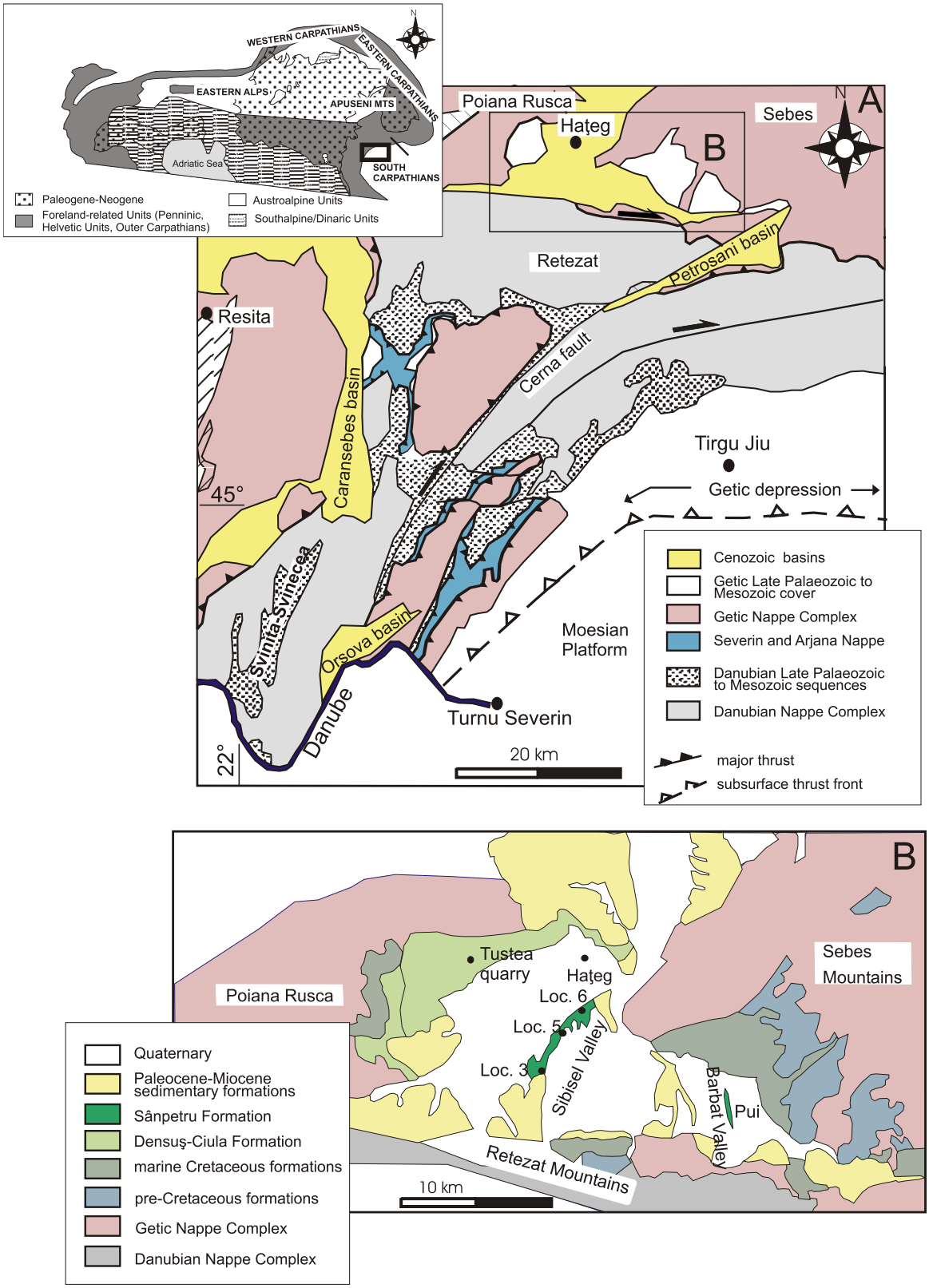

Fig. 1. A — Geological map of the study area; B — Haţeg basin — the distribution of the Ciula and Sânpetru formations are shown

al., 2002). Additional nesting sites were discovered during field work by Van Itterbeeck *et al*., (2004) and Smith *et al*., (2002). In the Haţeg basin, this faunal assemblage was discovered within terrestrial deposits of Maastrichtian age. At that time, the study area was situated at 27°N±5° (Panaiotu and Panaiotu, 2002) between two marine domains: the South Penninic to the north and the Tethys to the south (Camoin *et al*., 1993; Neubauer, 2002).

World-wide, the geological record suggests that the Cretaceous climate, generally described as "greenhouse climate", was much warmer than today, with minimal equator-to-pole thermal gradients (Amiot *et al*., 2004). The evidence for a warm Cretaceous climate includes the latitudinal expansion of vegetation provinces (Vakhrameev, 1991); the poleward migration of thermophilic organisms (e.g. Kauffman, 1973; Lloyd, 1982; Huber and Watkins, 1992); the expansion of dinosaurs into polar latitudes (Colbert, 1973; Olivero *et al*., 1991; Crame, 1992); and oxygen isotope determinations (Frakes and Francis, 1990; Huber *et al*., 2002). The Albian is characterized by a peak of warmth, followed by slight cooling/warming periods in the Late Cretaceous, and ending with a further cooling during Maastrichtian times (Barron, 1983; Arthur *et al*., 1988; Frakes and Francis, 1990; Frakes *et al*., 1992; Barrera, 1994; Clarke and Jenkins, 1999; Kuypers *et al*., 1999; Huber *et al*., 2002). Despite the temperature decline during the latter part of the Cretaceous, overall temperatures were still high compared to the Late Neogene.

Maastrichtian climate was not as warm and equable as the overall climate of the Cretaceous. The isotopic record from foraminifers and bulk sediments indicate temperature fluctuations during Maastrichtian time (Barron and Washington, 1984; Barrera, 1994; Barrera *et al*., 1997; Li and Keller, 1998; Clark and Jenkins, 1999; Huber *et al*., 2002). These fluctuations are represented by:

— progressive cooling during the lower Maastrichtian;

— accelerated cooling during the early to late Maastrichtian transition (70 to 71 Ma);

— abrupt warming at the end of Cretaceous (*ca*. 65.4 to 65.1 Ma) and subsequently temperature decrease during the last 100 k.y. of Maastrichtian.

Because ocean temperatures do not always reflect land temperatures, additional data are required in order to constrain continental palaeoclimatic conditions from the Haţeg basin at that time. Moreover, the general climate mode can be drastically influenced by local conditions (Ruddiman and Prell, 1997); therefore, efforts will be concentrated in order to understand the effects of late Cretaceous topographic changes (such as the uplift of metamorphic domes surrounding the basin area) on facies and climate distribution. The main objectives of this study are to characterize the Maastrichtian facies and palaeosols from the Haţeg basin, Romania, in order to get information about the conditions that controlled their formation and to have a better understanding of the environment and climate in which dinosaurs lived. For this purpose, field observations regarding the geometry of the deposits and their internal structures as well as mineralogical, geochemical analyses have been carried out from samples collected along representative profiles (Bojar *et al*., 2002, 2003).

GEOLOGY OF THE REGION

The southwestern South Carpathians represent a nappe pile, which is mainly composed of pre-Alpine basement nappes separated by the ophiolitic Severin unit (Fig. 1A). Tectonostratigraphically upwards, these units include:

— the Moesian platform with thick Lower Palaeozoic to Neogene deposits;

— the Danubian Nappe complex (exposed within the Danubian window) with a Cadomian/Variscan basement and Upper Palaeozoic to Mesozoic cover;

— the Severin flysch-and-ophiolite nappe;

— the Getic and the Supragetic nappes (both with Variscan basement and Mesozoic cover) (Berza *et al*., 1994; Kräutner, 1996).

The nappe assembly was completed during the Early to Late Cretaceous, and was mainly overprinted by Paleogene and Neogene wrenching along steep dextral strike-slip faults.

In the Haţeg region, the oldest deposits overlying the Getic basement are the Lower Jurassic continental clastic sediments, which shift gradually to Middle Jurassic marine limestones and marls. During Late Jurassic to Aptian time, reef and fore-reef limestones were deposited (Stilla, 1985). A major inversion took place around the end of the Aptian — beginning of the Albian when the whole area was exhumed and eroded, as indicated by bauxite deposits accumulated within the palaeokarst. Facies changes and erosion were related to closure of the Severin ocean, collision, and stacking of the Supragetic units on the top of the Getic tectonic units. This event, known as the Austrian phase (Sandulescu, 1984), was also documented by K-Ar, ^{40}Ar–^{39}Ar and fission-track dating (Grünfelder *et al*., 1983; Bojar *et al*., 1998; Dallmeyer *et al*., 1998; Willingshofer *et al*., 2001).

Within the Haţeg basin (Fig. 1B), the Upper Cretaceous sequences were divided by Stilla (1985) into sedimentary groups, separated by local unconformities. Upper Albian (Vraconian)–middle Turonian sedimentary units are represented by conglomerates, sandstones and marls, with sedimentation starting under continental conditions and shifting progressively to a marine facies. The Turonian–lower Coniacian sandstones and mudstones follow, above a sedimentary gap. The middle Coniacian, Santonian and Campanian successions are represented by a proximal flysch facies with sandstones, conglomerate lenses, marls and mudstones, which indicate progressive deepening of the basin and establishment of an open marine environment. Two different continental formations of Maastrichtian to Lower Paleogene age are known: the Densuş-Ciula and the Sânpetru Formations both representing molasse type deposits. The Late Cretaceous basin subsidence correlates with the stacking of the Getic Nappe on the top of the Danubian realm, as well as uplift of the surrounding areas and orogenic collapse (Bojar *et al*., 1998; Willingshofer, 2000; Willingshofer *et al*., 2001). In a regional framework, this phase corresponds to the Laramian orogeny (Sandulescu, 1984). The basin is bordered to the north-west of the Pui locality, as well as to the south, by faults crosscutting the Maastrichtian strata. Subsidence within the Haţeg basin and uplift within the Danubian realm continued also during Oligocene time, as recorded by the sedimentary formations disposed on the southern border of the Haţeg basin (e.g. Clopotiva Conglomerate). Burial of the Maastrichtian strata by younger deposits was limited to a few hundred metres.

STRATIGRAPHY AND DISTRIBUTION OF THE MAASTRICHTIAN DEPOSITS

As our study focuses on facies and palaeoenvironment reconstruction during late Maastrichtian time, the stratigraphy of these deposits will be discussed in more detail.

The Densuş-Ciula Formation crops out in the northwestern part of the basin and it is divided into three sub-formations, with a total thickness of nearly 4 km (Anastasiu and Csobuka, 1989; Grigorescu *et al*., 1990*a*). The Lower Densuş-Ciula Sub-formation contains volcano-sedimentary sequences interlayered with lacustrine marls, which lie discordantly on uppermost Campanian flysch deposits (Grigorescu and Melinte, 2001). The Middle Densuş-Ciula Sub-formation with a total thickness of 2 km, is represented by matrix-supported conglomerates, cross-bedded sandstones and massive red, brown and green-grey mudstones. These mudstones contain fossil dinosaur eggs, bones, teeth, multituberculate remains, mollusc shells and plants (Nopcsa, 1923; Grigorescu *et al*., 1990*a*, *b*; 1994; 1999). The Maastrichtian age is indicated by fresh water gastropod assemblages including *Bauxia bulimoides*, *Gastrobulimus munieri*, *Rognacia abreviata*, *Ajkaia* cf. *gregaria*, and palynological assemblages, with *Pseudopapilopollis praesubhercynicus* (Antonescu *et al*., 1983; Pana *et al*., 2002). Pana *et al*. (2002) describe a very large assemblage of freshwater gastropods including 30 species from 12 families from both the Sânpetru and Densuş-Ciula formations. The dinosaur assemblage includes *Magyarosaurus dacus*, *Zalmoxes robustus*, *Zalmoxes shqiperorum*, *Telmatosaurus transsylvanicus*, *Euronychodon* (Grigorescu and Csiki, 2002; Weishampel *et al*., 2003). The probably Paleogene deposits of the Upper Densuş-Ciula Sub-formation are devoid of volcanoclastic material, as well as of dinosaur remains.

The Sânpetru Formation crops out mainly along the Râul Mare and Sibişel valleys. Preliminary magnetostratigraphy for the Sânpetru Formation, upstream of the point called La Scoaba, corresponding to location 6 in our study, suggests that the sedimentation, with two short intervals of normal polarity, started at the end of chron C32n (probably <72 Ma) (Panaiotu and Panaiotu, 2002). All the other palaeomagnetic sites distributed upstream, for more than 4 km, until the upper limit of this formation, have only reversed polarity and the corresponding time interval is probably chron 31r, between 68.7 and 71.0 Ma (Cande and Kent, 1995). The mean palaeolatitude of the Haţeg basin during this period is best estimated from palaeomagnetic results obtained from contemporaneous magmatic activity: 27°N±5° (Pătraşcu *et al.*, 1992; Panaiotu, 1998). The Sânpetru Formation is almost devoid of coarse volcanoclastic deposits; dinosaur bones are frequently found here either including: *Magyarosaurus dacus*, *Zalmoxes robustus*, *Zalmoxes shqiperorum*, *Telmatosaurus transsylvanicus*, *Struthiosaurus transsylvanicus*, *Euronychodon* and dromaeosaurids (Grigorescu and Csiki, 2002; Weishampel *et al*., 2003). Mammal remains were found within this formation as well (Grigorescu *et al*., 1985; Smith *et al*., 2002). From location 3 of this study, the following palynological assemblage has been determined (Ana Danis, 2005 pers. comm.): *Oculopollis sibiricus* Zaklynskaya, *O*. cf. *solidus* Zaklynskaya, *O*. cf. *parvoculus* Goczan, *Trudopollis* sp., *Semioculopollis* cf. *praedicatus* Kutzch, confirming the Maastrichtain age of the deposits.

The facies distribution is interpreted as indicating deposition in an ancient braided fluvial system (Grigorescu *et al*., 1990*a*).

In the Haţeg basin, the transition from Maastrichtian to Lower Paleogene deposits (mostly represented by conglomerates) is inaccessible; therefore no direct observation regarding this interval could be made.

METHODS AND MATERIAL STUDIED

The granulometric distribution was studied by combining wet sieving and automatic sedimentation analysis with the *Sedigraph 5000 ET*. For this purpose 50 g of dry sample was treated for 24 hours with 200 ml 10% H_2O_2 in order to oxidize the organic matter and to disintegrate the sample. The sample was then cleaned in an ultrasonic bath and sieved using 2 mm, 630 μm, 200 μm, 63 μm and 40 μm meshes. The fraction coarser than 40 μm was dried and weighed. Calgon 0.05% was added to the fraction finer than 40 μm, which was afterwards dispersed in an ultrasonic bath, and analyzed with X-rays in the *Sedigraph*.

The samples were studied by X-ray diffraction (XRD) using a *Philips 1710* diffractometer with an automatic divergent slit, 0.1° receiving slit, Cu LFF tube 45 kV, 40 mA, and a single-crystal graphite monochromator. The measuring time was 1s in step-scan mode and step size of 0.02°. Bulk samples as well as the clay fractions (<2 μm) were analyzed. Sample preparation generally followed the methods described by Whittig (1965) and Tributh (1991). Dispersion of clay particles and destruction of organic matter was achieved by treatment with dilute hydrogen peroxide. Separation of the clay fraction was carried out by centrifuging. The exchange complex of each sample (<2 μm) was saturated with Mg and K using chloride solutions by shaking. As in the methods of Kinter and Diamond (1956), the preferential orientation of the clay minerals was obtained by

Table 1

Grain size distribution of palaeosols [in mass %]

Location	Sample	Gravel	Sand	Silt	Clay
Tuştea	m01	0.4	14.7	60.8	23.9
	m4.2.1	–	13.5	49.2	37.3
	m4.2.3	–	45.9	39.7	14.5
	m4.4.1	–	24.5	45.3	30.3
Bărbat V.	74	3.5	69.8	22.2	4.5
	70	0.1	34.9	48.6	16.5
	70a	3.4	19.5	56.6	20.6
Location 6 Sibişel	92	3.8	12.5	67.1	16.6
	94	28.4	4.5	53.0	14.1
Location 5 Sibişel	96	23.7	11.7	44.6	20.0
Location 3 Sibişel	85	84.1	6.0	7.4	2.5

suction through a porous ceramic plate. To avoid disturbance of the orientation during drying, the samples were equilibrated over 7 days in saturated NH_4NO_3 solution. Afterwards expansion tests were made, using ethyleneglycol, glycerol and DMSO (Dimethylsulfoxide) as well as contraction tests by heating the samples up to 550°C. After each step the samples were run from a 2θ angle of 2 to 40 E.

The clay minerals were identified according to Thorez (1975), Brindley and Brown (1980), Moore and Reynolds (1997), and Wilson (1989). Semi-quantitative estimations of the clay mineral composition were carried out using the corrected intensities of characteristic X-ray peaks (Riedmüller, 1978). The semi-quantitative mineral composition of the bulk samples was estimated using the method described by Schultz (1964).

FTIR (Fourier Transformed Infrared Spectroscopy) was done on a Perkin Elmer Paragon 500 instrument. The sample (1 mg) was powdered with 200 mg KBr. This mixture was pressed to a disk of 10 mm diameter. The sample chamber was purged with dried N_2. The resolution of the measurements was 2 cm^{-1}. The analyses were performed between 400 and 4000 cm^{-1}

Isotopic analyses of carbonates were performed using an automatic *Kiel II* preparation line and a *Finnigan MAT Delta Plus* mass spectrometer. The reaction with H_3PO_4 was carried out at 70°C. NBS-19 and an internal laboratory standard were analyzed continuously for accuracy control; standard deviation (1σ) was 0.1‰ for $\delta^{18}O$ and 0.06‰ for $\delta^{13}C$. All isotopic results are reported in per mil, relative to the Pedee Belemnite standard (PDB) for carbon and Standard Mean Oceanic Water for oxygen.

Cathodoluminescence was done using an *Citl Cold Cathodoluminescence 8200 mk3* electron gun, a vacuum chamber with windows and stage X-Y movement. The stage is coupled to a *Olympus BH-2* optical microscope. The measurement conditions are 17kV and 450mA.

For granulometry, bulk and clay mineralogy, 11 samples from Tuştea, Bărbat Valley and Sibişel were analyzed (Tables 1 and 2). A total of 113 carbonate concretions were cut and only calcite drilled from the central part of the concretion was used for stable isotopic analysis (Table 3). Eggshell fragments were cleaned in ultrasonic bath and sampled using a 0.5 mm drill.

FACIES DISTRIBUTION AND PALAEOSOL FEATURES

For each site, the data will be presented as follow: field observations on facies, granulometry, bulk and clay mineralogy as well as stable isotopic composition of calcretes.

At Tuştea quarry (Figs. 2 and 3A) the 10 m vertical escarpment comprises two levels of massive red mudstones intercalated with conglomerates and cross-bedded sandstones. The bottom of the sequence is represented by a massive red mudstone followed by 4 metre-thick coarse-grained, poorly sorted sandstones and conglomerates with massive to trough cross-bedding. The deposits show massive bedding to laterally crosscutting and alternating poorly sorted sandstones and conglomerates, which indicate unstable channelized flow with discharge fluctuations. The coarse facies is interpreted as deposited in an alluvial channel. The inter-channel areas, starved of coarse sediment supply, were sites of pedogenesis (Fig. 3B, C). The soils show: a red mud horizon with blocky structure characterized by the presence of well developed vertical roots and burrows (Fig. 3C), and a horizon with calcareous concretions (Fig. 3B). There are 7 levels of calcretes with thickness and lateral continuity indicating moderately developed soils (Retallack, 2001). Granulometric analyses show that the main grain size fraction is silt (Table 1); only sample m4.2.3 is dominated by sand. The clay fraction is the second frequent, with values between 14.5 and 37.3%. Up to a few percent of quartz and calcite are present in all samples. Feldspar is generally more frequent than quartz and calcite. In the fraction less than 2 μm, smectite, a swelling clay mineral, dominates with up to 94 mass percent (Fig. 4a). Other clay minerals are present in very small amounts: illite is in the range of 4 to 10 mass percent, and kaolinite 2 to 4 mass percent. Trace chlorite could be detected in just one sample (Table 2). FTIR analysis of the less than 2 μm smectite fraction shows that the mineral is a montmorillonite (Fig. 4b). As the most prominent pedogenic feature is the presence of the calcic horizon the soils can be classified as calcisols (Mack and James, 1993). The soils do not show erosion by later deposits; rather they vertical aggradations due to slow deposition of fine material and progressive burial, this pedofacies type being known as multiple buried soils (Daniels, 2003). The only levels

Table 2

Clay mineralogy of the clay fraction < 2μm [in mass %]

Location	Sample	Smectite	Illite	Chlorite	Kaolinit	Mixed layer
Tuştea	m01	89	7	–	4	–
	m4.2.1	91	7	–	2	–
	m4.2.3	94	4	–	2	–
	m4.4.1	86	10	traces	4	–
Bărbat V.	74	43	34	23	–	traces
	70	57	30	9	4	traces
	70a	40	37	14	9	–
Location 6 Sibişel	92	68	16	16	–	–
	94	55	20	25	–	–
Location 5 Sibişel	96	54	15	31	–	–
Location 3 Sibişel	85	46	24	30	–	–

Table 3

Stable isotopic composition

Location	Sample	Sample description	^{18}O (SMOW)	^{13}C (PDB)
1	2	3	4	5
Tuştea	ma1	mudstone (calcite cement)	26.7	–6.8
	ma2	mudstone	24.1	–8.2
	ma3	mudstone	24.2	–8.2
	ma4	mudstone	24.2	–7.6
	m4.1	mudstone	19.4	–14.6
	m4.2.2	mudstone	23.7	–7.4
	m4.3	mudstone	23.2	–8.4
	m4.2.2	mudstone	23.7	–7.4
	m4.3	mudstone	23.2	–8.4
	egg1	dinosaur egg, calcite	29.8	–13.8
	egg1a	egg	29.9	–13.7
	egg2	egg	30.8	–14.1
	egg2a	egg	30.5	–14.1
	egg3	egg	29.5	–13.3
	egg3a	egg	29.6	–12.6
	egg2	egg	30.1	–14.6
	egg2	egg	29.9	–14.2
	egg2	egg	30.3	–15.0
	CO3	calcrete	24.6	–8.6
	CO3	calcrete	24.6	–8.6
	CO2	calcrete	24.8	–8.5
	CO1	calcrete	24.4	–8.5
	c2.1	calcrete.	24.7	–8.3
	m2.1	calcrete	25.0	–8.6
	c2.2	calcrete	24.5	–8.7
	c4.1	calcrete	24.1	–8.3
	c4.2.1	calcrete	24.7	–8.1
	c4.2.2	calcrete	24.8	–8.2
	c4.3.1	calcrete	24.7	–8.5
	c4.3.2	calcrete	24.4	–9.0
	c4.3.3	calcrete	24.9	–8.3
	c4.4.1	calcrete	24.9	–8.2
	c4.4.2	calcrete	24.6	–8.5
	c5.2-2003	calcrete	24.3	–8.5
Bărbat Valley	46.1/red	calcrete	24.4	–8.0
	46.2/red	calcrete	23.7	–7.1
	47.1	calcrete	23.7	–7.2
	47.2	calcrete	24.4	–7.9

where erosion can be seen is at the contact with the massive to cross-bedded sandstones.

From some of the carbonate concretions, thin sections were studied under cathodoluminescence, a powerful technique to distinguish secondary diagenetic effects. Microscopic examination of thin sections using cathodoluminescence revealed a brown, non-luminescent massive micritic groundmass, throughout which detrital grains of feldspar and quartz are dispersed. The carbonates show a narrow range of isotopic compositions, with $\delta^{18}O$ isotopic values between 24.1 and 25.0‰ (SMOW) and $\delta^{13}C$ between 8.1 to –8.9‰ (PDB) (Fig. 2 and Table 3).

Associated with one of the concretion layers, just above it, dinosaur nesting sites together with embryonic/hatchling skeletal remains were found (Fig. 2). Based on these remains, the eggs are thought to belong to a hadrosaurid, *Telmatosaurus transsylvanicus* (Grigorescu, 1993). Scanning electron micrographs and study of thin sections under polarized light indicate that the internal multistratified growth structure of the eggs as well as the external structure has been entirely preserved (Fig. 5A, B, C). Cathodoluminescence revealed a brown, non-luminescent mass (Fig. 5D). Further evidence, which supports that the initial isotopic ratios of the eggshells were not affected by diagenesis, is that the $\delta^{18}O$ and $\delta^{13}C$ of the shells are different than those of the associated matrix, which has a similar isotopic composition to the calcretes (Table 3). This would be unlikely if any significant alteration had affected the eggs because such effects tend to homogenize the isotopic composition between shells and matrix. The eggshells reveal $\delta^{18}O$ values between 29.5 and 30.5‰ (SMOW) and $\delta^{13}C$ between –13.0 and –14.0‰ (PDB).

The section along the Bărbat Valley, south of the Pui locality, displays parallel laminated mudstones with numerous levels of concretions. Along the Bărbat Valley, the strata are horizontal or dip at a few degrees towards the south. A profile opened some hundred metres along the valley is shown in Figure 6. The vertical thickness of the profile is approx. 22 m. The profile was accessible in 2003, during a summer with low amounts of precipitation. In 2004, during a year with high amounts of precipitation, the profile was almost covered by recent alluvial sediments or water. Along the riverbed,

Tab.3 continued

1	2	3	4	5
Bărbat Valley	47.3	calcrete	23.9	–7.0
	48.1	calcrete	23.9	–6.6
	48.2	calcrete	24.3	–7.3
	49	calcrete	24.2	–7.5
	50.1	calcrete	23.9	–6.4
	50.1	calcrete	24.0	–6.5
	51.1	calcrete	24.1	–5.8
	51.1	calcrete	23.9	–5.9
	52.1	calcrete	24.0	–5.8
	52.2	calcrete	24.3	–4.8
	53.1	calcrete	24.5	–8.1
	53.2	calcrete	24.0	–6.5
	54.1	calcrete	24.2	–5.9
	54.1	calcrete	24.0	–5.9
	69	calcrete	24.0	–6.1
	71	calcrete	24.1	–5.7
	75	calcrete	24.1	–7.4
	76	calcrete	24.0	–6.7
	77	calcrete	24.2	–8.5
	78	calcrete	24.3	–6.7
	80	calcrete	24.3	–7.3
	81	calcrete	23.9	–6.9
	82	calcrete	24.2	–5.5
	56.1	calcrete	27.1	–7.4
	56.2	calcrete	27.1	–7.4
Location 3 Sibişel Valley	5	calcrete	21.5	–9.4
	7	calcrete	22.0	–8.7
	9	calcrete	23.3	–15.4
	9	calcrete	22.6	–14.2
	31.1	calcrete	23.5	–9.0
	31.1	calcrete	23.4	–9.2
	31.2	calcrete	23.7	–11.2
	31.2	calcrete	23.1	–11.2
	31.3	calcrete	23.5	–8.9
	31.3	calcrete	23.6	–-8.8
Location 5 Sibişel Valley	10.1	calcrete	22.8	–10.6
	10.2	calcrete	22.8	–10.6
	10.2	calcrete	23.5	–10.2
	32.1	calcrete	19.4	–15.7
	32.2	calcrete	20.0	–15.8
	35.1	calcrete	24.3	–9.6
	35.1	calcrete	23.6	–10.6

the outcrops are generally small; therefore, no further observations could be made about the structures or the geometry of the sand bodies. The facies are represented by coarse sandstones to conglomerates and alluvial plain deposits with palaeosols. Characteristic is the presence of a red horizon with parallel lamination, a level with calcareous concretions underlain by a red horizon with parallel lamination and drab-haloed traces in the lower part (Fig. 6). The drab-haloed traces found here are approximately 1–2 cm diameter and have a higher density than at Tuştea. The palaeosols are characterized by the presence of calcrete intervals up to 40 cm thick, locally better developed than at Tuştea. As the most striking feature is the development of a concretion level, the palaeosoils can be classified as calcisols. Locally the calcrete horizon is missing but this may reflect short episodes characterized by higher depositional rates. Generally the pedofacies varies from cumulic to buried soil profiles (Daniels, 2003). Granulometric data show that sand is the dominant fraction for sample 74, while for the soil levels (samples 70 and 70a) silt and subordinate clays are the main components. Small amounts of quartz and feldspars and traces of calcite are present in all samples. At Bărbat Valley all samples contain small amounts of gravel, and the clay content is generally lower than at Tuştea. Smectite is again the most frequent clay mineral, in the range of 40 to 57 mass percent. Illite becomes more frequent than at Tuştea, and shows values of up to 37 mass percent. Chlorite is also present in the clay fraction (9–23 mass percent), the amount of kaolinite being low (Table 2).

The $\delta^{13}C$ isotopic composition of the calcretes (Fig. 7) varies between –8.0 to –5.0‰ (PDB). The $\delta^{18}O$ values range between 23.6 to 24.5‰ (SMOW), being ~ 0.5‰ lighter than the isotopic signature of the calcretes from Tuştea quarry.

The Sânpetru Formation crops out mainly along the Sibişel and Râul Mare valleys. Detailed mapping of the sequences and the facies developed in the Sibişel Valley are shown in Figures 8–10. The valley opens from the centre of the basin towards the south, a profile with progressively younger deposits, with the vertical thickness reaching approximately 2 km. Three different locations along the valley will be described, firstly in terms of the general character of the facies development, and secondly as regards the soils developed at each location. At locations 5 and 6, sand bodies with trough

Tab.3 continued

1	2	3	4	5
Location 5 Sibişel Valley	35.2	calcrete	23.2	–12.5
	35.2	calcrete	23.5	–12.3
	35.1	calcrete	23.4	–10.2
	35.2	calcrete	23.4	–10.2
	36.1	calcrete	23.9	–11.1
	36.1	calcrete	24.0	–11.1
	38	calcrete	23.1	–9.1
	39.1	calcrete	23.0	–10.1
	39.2	calcrete	23.2	–12.8
	39.3	calcrete	23.1	–9.8
	40.2	calcrete	23.2	–10.9
	40.3	calcrete	23.3	–11.3
	40.3	calcrete	23.1	–11.3
	41.1	calcrete	23.4	–8.3
	41.1	calcrete	22.7	–9.6
	41.2	calcrete	23.2	–8.4
	41.3	calcrete	23.1	–8.2
	42.1	calcrete	22.7	–8.2
	42.2	calcrete	22.7	–8.8
	42.3	calcrete	22.8	–8.7
	43	calcrete	23.2	–8.6
	44.1	calcrete	21.2	–8.7
	44.2	calcrete	22.6	–9.1
	45.1	calcrete	22.8	–8.3
	45.2	calcrete	22.7	–8.3
	45.3	calcrete	22.8	–8.0
Location 6 Sibişel Valley	18.1	calcrete	23.1	–9.0
	18.2	calcrete	23.0	–9.40
	18.3	calcrete	23.9	–11.3
	18.4	calcrete	24.1	–11.1
	20	calcrete	22.7	–8.4
	22	calcrete	22.9	–9.4
	22.8	calcrete	22.9	–10.3
	22.9	calcrete	22.9	–10.2
	22.10	calcrete	23.8	–10.1
	25.1	calcrete	24.9	–11.8
	25.2	calcrete	24.3	–10.4
	25.3	calcrete	23.1	–11.4
	27.1	calcrete	24.2	–7.7
	27.2	calcrete	23.7	–7.9
	29.1	calcrete	21.5	–8.4
	29.2	calcrete	21.1	–8.8

cross-bedding occur (Fig. 9A, B). These were deposited in channels isolated in floodplain sediments. The lateral wings of sand and silt represent levees, which extend laterally into overbank fines (Mjos *et al.*, 1993). The channel bottom is characterized by erosional surface and the presence of various clasts. Besides the channel facies, sheets of sandstones up to 1 m thick with parallel bedding were also observed. The bottom of the sand bodies show little erosion and are laterally associated with channels. Couplets of up to 0.5 m thickness of sandstones and mudstones are also present. The sandstones usually have sharp bases showing no significant erosion, and gradational tops fining upwards into the mudstone-dominated part. Towards location 5, the thickness of the channel and sand-rich units increases. The amount of gravel increases towards location 3, where channels with massive to cross-bedded conglomerates and sandstones are also present (Fig. 9C). For the mudstone-rich units, silt is again the dominant grain size fraction for all the three outcrops; the content of sand and clay fraction being generally low (Table 1). Clay minerals are present in all samples but they are less frequent than in the previous profiles investigated. In contrast, feldspars become more frequent and are detectable in all samples in significant amounts. Calcite is only present in trace amounts, except in sample 85 where higher were detected.

At location 6, the alluvial plain shows palaeosols for which the following horizons may be distinguished: a red horizon with parallel lamination, a level with moderately to well-developed concretions (up to 10 cm diameter) underlain by parallel-stratified mudstones, the colour of which changes progressively from red to mottled textures involving grey-green and red (Fig. 10A). Drab haloes are also present. Compressional structures, formed during wetting and drying of soils rich in swelling clays (Duchafour, 1982), are also observed (Fig. 10B). Under the microscope, the concretions show a micritic texture (Fig. 10C). The palaeosols from this location are similar to those along the Bărbat Valley, showing buried profiles although strongly developed concretion levels, indicating cumulic profiles, are lacking. As in the Bărbat Valley, there are palaeosol levels with missing calcrete horizons. Thus the type of palaeosoils from this outcrops is dominated by calcisols, only sporadically vertisols without a calcic horizon are present. The clay content is

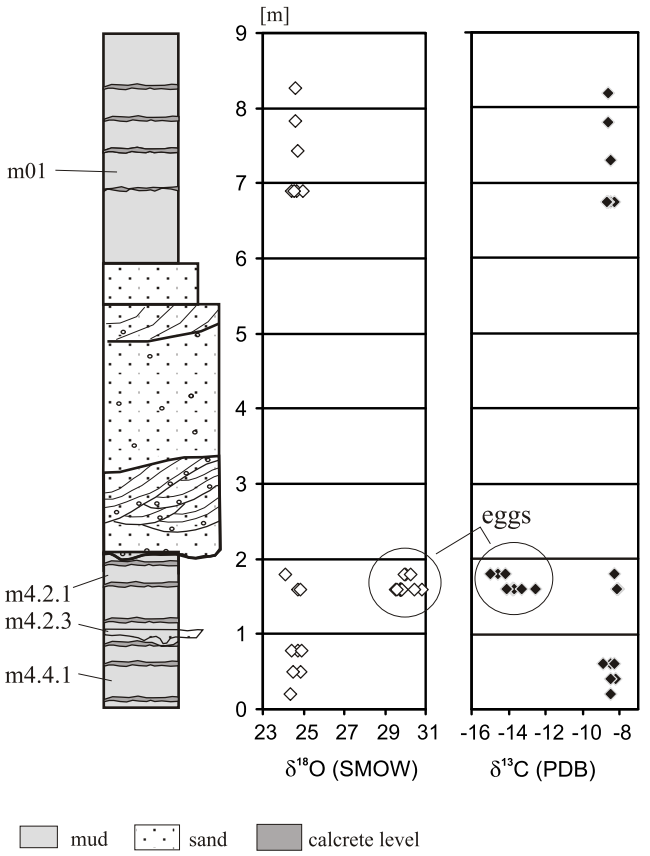

Fig. 2. Facies distribution at Tuştea quarry and stable isotopic composition of calcretes, mudstones and dinosaur eggs from Tuştea quarry

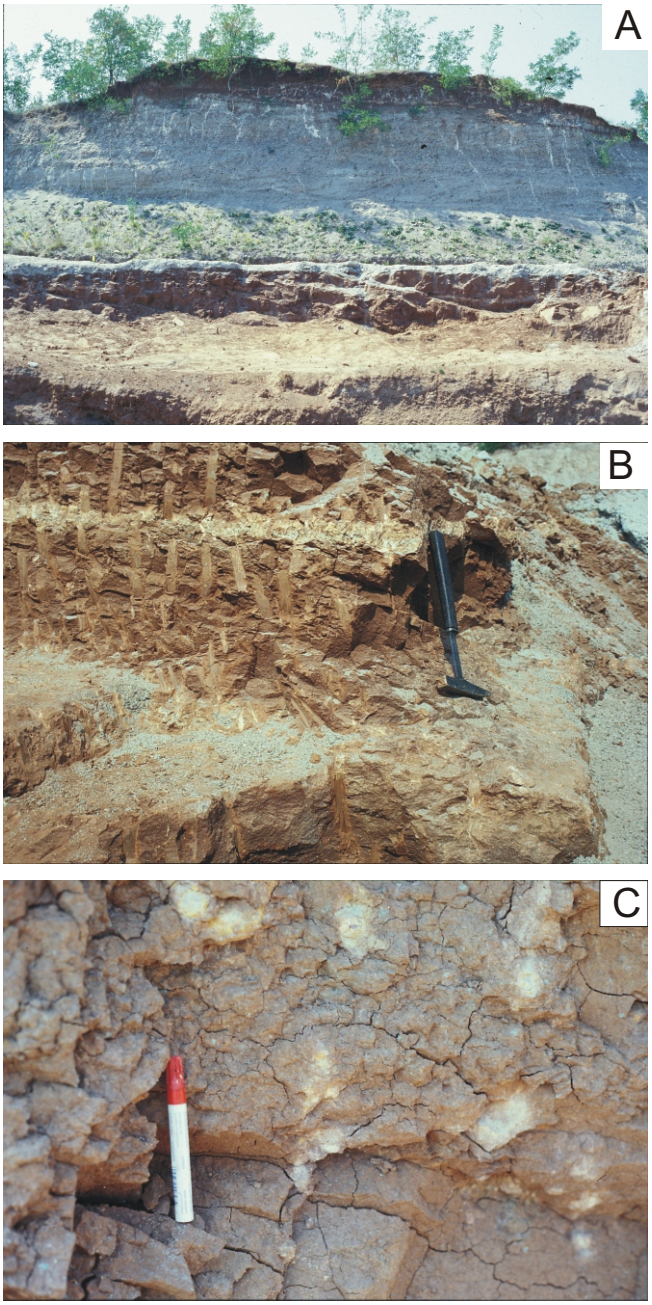

Fig. 3. A —Tuştea quarry, frontal view; B — calcrete level; C — well developed vertical roots

lower, although the mineral composition is similar to that in the Bărbat Valley. Smectite is the most frequent clay mineral, comprising 55 to 68 mass percent, subordinate chlorite and illite being also present. Progressively, towards location 5, the predominant type of palaeosol changes from calcisols to vertisols. At location 5 and 3, palaeosols show the following horizons from top to bottom (Fig. 10D): organic rich grey-green mudstones, a mudstone level, and a calcrete level underlain again by grey-green mudstones. Variations from this type of soil occur, as the organic-rich or the calcrete layer are locally missing. At location 3, the amount of chlorite and illite exceeds that of smectite (Fig. 4c).

Along the valley, toward the top of the sequence, the oxygen isotopic compositions show a shift towards lower values, from around 24.0‰ at location 6 to values around 22.0–23.0‰ at location 5 and 3. The carbon isotopic compositions show values between –8.0 and –11.0‰ at location 6 and higher variability and generally lower values at locations 5 and 3.

DISCUSSION AND CONCLUSIONS

The Middle Densuş-Ciula Sub-formation is well represented at Tuştea quarry, with massive red muds, palaeosols and sandstone/conglomerate intercalations. The Sânpetru facies is dominated by the development of fluvial deposits, as described along the Sibişel Valley. In fact, the two formations represent the "end members" of a transition between:

— a facies dominated by the development of an alluvial plain with low sedimentation rates and frequent palaeosol levels,

— a facies dominated by the presence of alluvial channels and adjacent alluvial plain.

Generally the fluvial facies are found in the centre and the southern border of the basin.

At Tuştea, the red colour and the presence of calcretes with a micritic texture indicate that the soils formed above the water table under oxidizing, alkaline conditions (Retallack, 1991). These conditions were favourable for the preservation of egg and bone material (Krumbein and

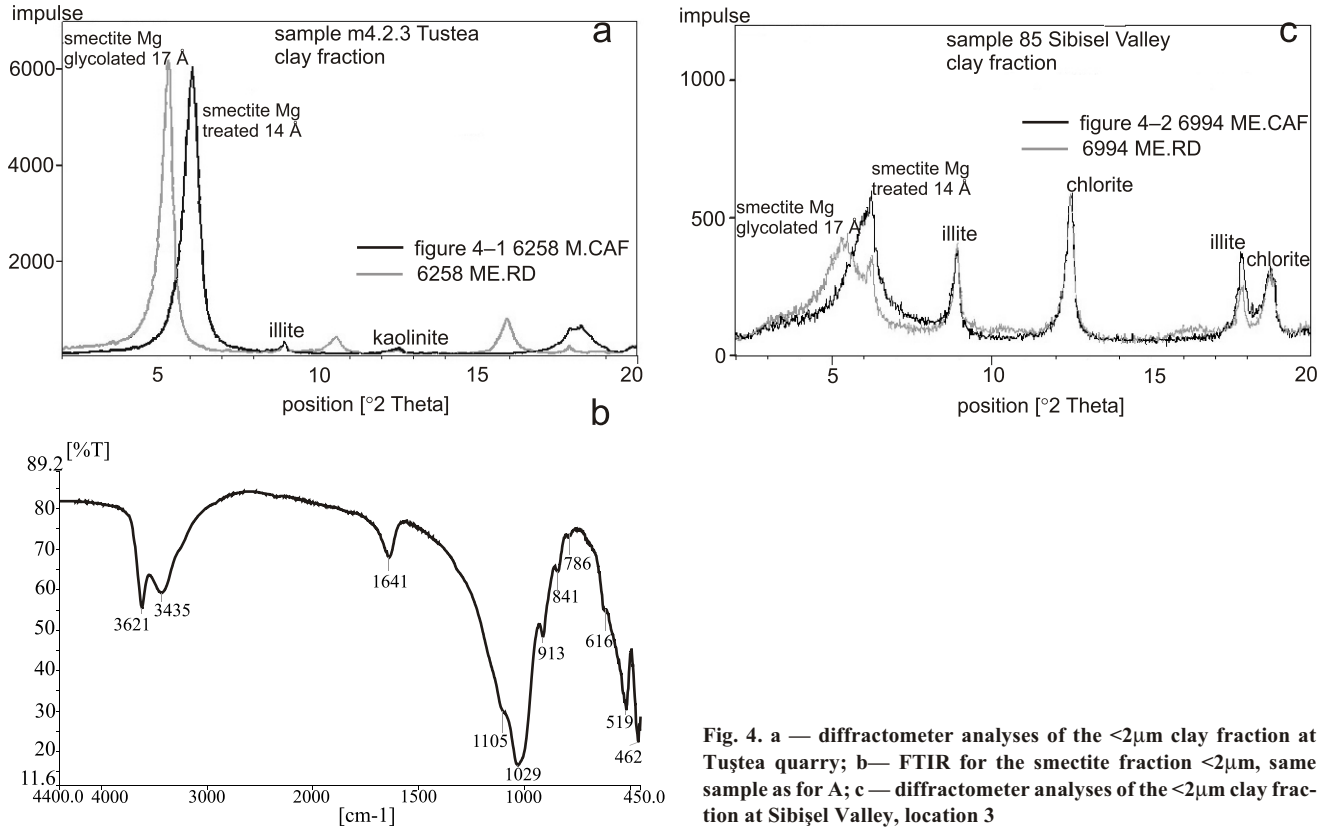

Fig. 4. a — diffractometer analyses of the <2μm clay fraction at Tuştea quarry; b— FTIR for the smectite fraction <2μm, same sample as for A; c — diffractometer analyses of the <2μm clay fraction at Sibişel Valley, location 3

Garrels, 1952). The well-developed vertical root traces also suggest well-drained soils. The thickness and distribution of the calcrete horizons indicate a succession of buried, moderately to strongly developed soils (Retallack, 1998). As there are no lateral outcrops, observations related to the geometry of the sand body are limited. The position of the outcrops, not far from the northern border of the basin, the good drained palaeosols indicating a higher, terrace position as well the structure and granulometry of the sand body described, support rather deposition from an alluvial fan, feeding the basin (Stanistreet and McCarthy, 1993). The high content of smectite (montmorillonite), up to 98 mass percent, indicates alteration of basic rocks. The basic material may be of volcanoclastic origin related to the to banatitic volcanism then active in the South Carpathians. The volcanoclastic material may be reworked, for example from the Lower Densuş-Ciula Sub-fomation, situated some 20 km northwestwards.

The sequences along the Bărbat Valley were deposited at the margin of an alluvial plain. Palaeosols are characterized by high maturity indicating distal position with respect to the main active channels. The drab-haloes are interpreted to have formed in periodically waterlogged soils, by anaerobic bacterial activity in stagnant water around roots (Retallack, 2001). Concerning this outcrops, we obtained similar results as did Van Itterbeeck *et al*. (2004), although the two studies were carried out independently. We would rather interpret the sequence not as well drained (Van Itterbeeck *et al*., 2004) but as periodically waterlogged, as indicated by the presence of the drab haloes. This feature suggests a higher position for the water table and periodic fluctuations. The lesser amount of smectite could be related to the lower availability of volcanoclastic material.

On Sibişel Valley, the high proportion of sandstones and mudstones, as well as the outcrop geometry, indicate a river facies with a low flow gradient and deposition in relatively shallow channels. The disposition of the channels within the outcrop indicates frequent avulsion events. The sandstone-mudstone couplets are interpreted as formed during individual flood events. Each couplet represents a rising flood stage and subsequent falling stage with deposition of silt and clay. The soils found at location 6 are weakly to moderately developed, although similar to those described along the Bărbat Valley. The progressive decrease in the soil maturity from Bărbat to Sibişel is related to different sedimentation rates at the two sites and to the more distal position of Bărbat Valley outcrops relative to the channel belt. The absence of calcretes within some of the palaeosol levels may be related to short episodes of higher depositional rates. Along the Sibişel Valley, besides the difference in maturity between the two already-mentioned sites, there are also changes in palaeosol type. The general character changes from generally well-drained, periodically water-logged soils (location 6) towards soils indicating rather stagnant water conditions (locations 5 and 3). At locations 5 and 3 the general reducing conditions and the lack of oxygen favored accumulation of an organic-rich layer at the top of some palaeosols. The facies distribution indicates that the weakly- to moderately-developed hydromorphic palaeosols formed close to the active channel belt. The massive channel conglomerates at location 3 indicate catastrophic flooding

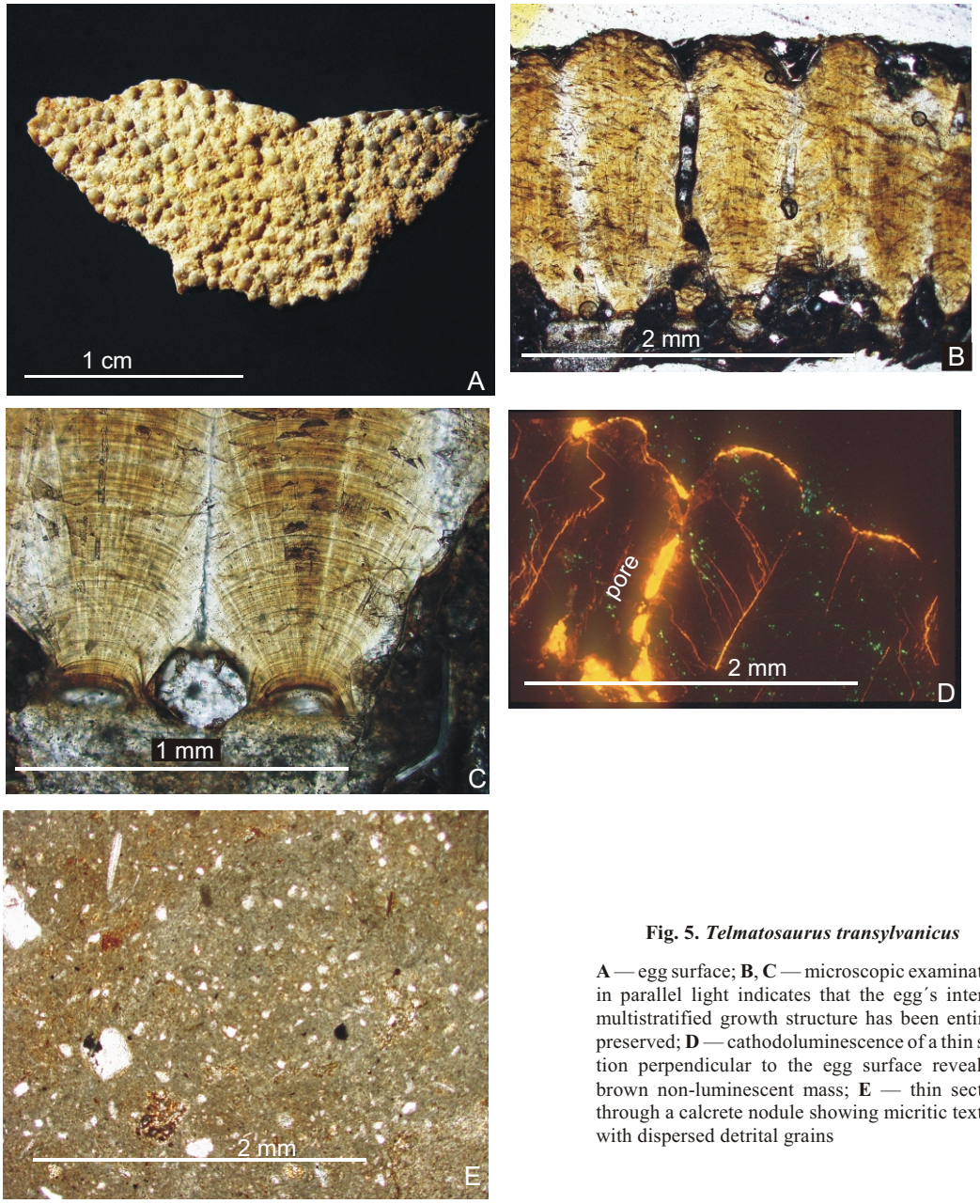

Fig. 5. ***Telmatosaurus transylvanicus***

A — egg surface; **B**, **C** — microscopic examination in parallel light indicates that the egg´s internal multistratified growth structure has been entirely preserved; **D** — cathodoluminescence of a thin section perpendicular to the egg surface reveals a brown non-luminescent mass; **E** — thin section through a calcrete nodule showing micritic texture with dispersed detrital grains

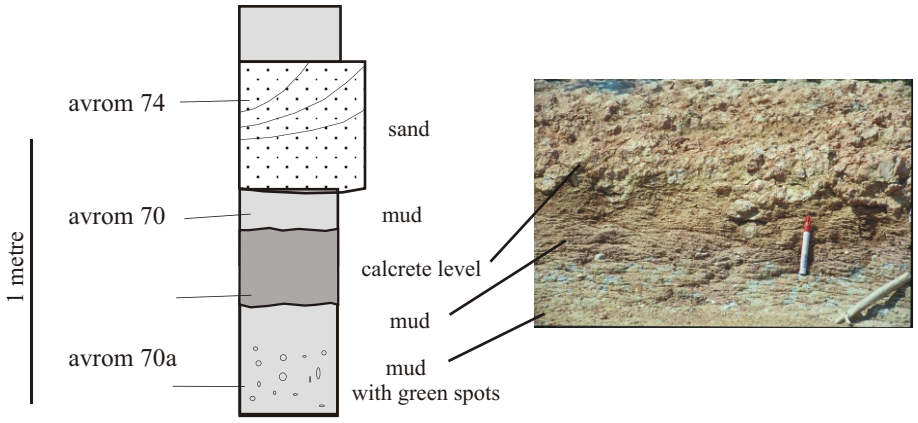

Fig. 6. Typical profile from the Bărbat Valley

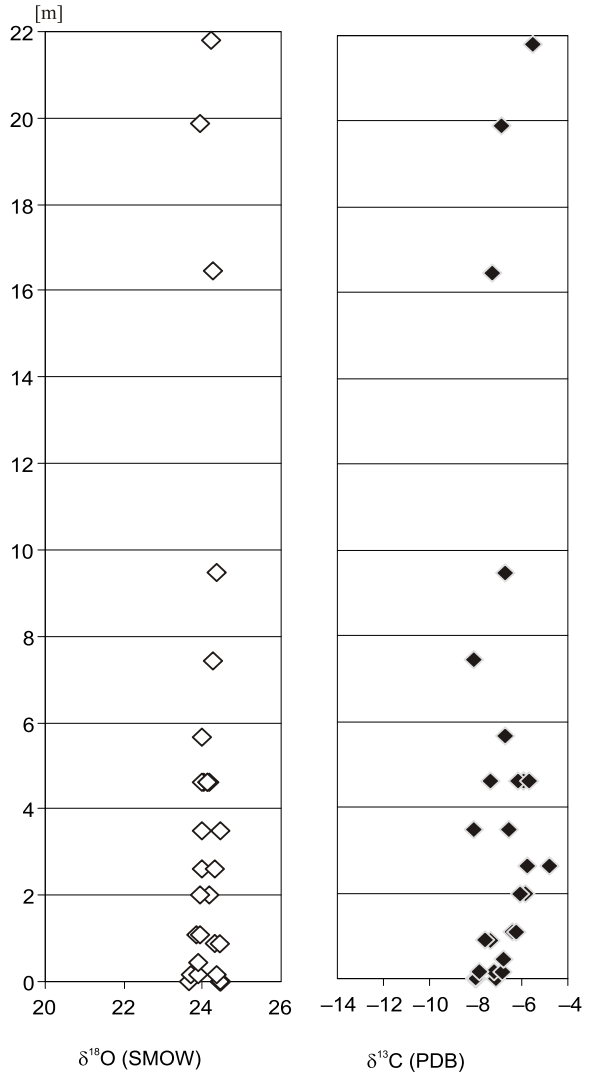

Fig. 7. Stable isotopic composition of calcretes along the Bărbat Valley

events, possibly enhanced by uplift of the surrounding mountains. Unstable tectonic conditions are also suggested by the change in clay mineralogy from smectite- to illite-chlorite dominated as well by an increase in minerals indicating erosion from crystalline substrates rich in quartz and feldspar (Chamley, 1989). In conclusion, the general trend towards the top of the sequence points toward an increase in sedimentation rates and a change from relatively stable tectonic conditions to more unstable ones.

The distribution of the fluvial facies, within the centre and the southern border of the basin may represent the result of channel forcing into more rapidly subsiding areas of the floodplain during Maastrichtian times. The facies distribution, palaeosol similarities and the similarities in isotopic composition of the calcretes support a similar age for the Tuştea and ărbat profiles and location 6 on Sibişel Valley. Palaeomagnetic data indicate that the sequences along the Sibişel Valley were deposited during chron C32-31; for the other two profiles no palaeomagnetic information is yet available.

INDICATORS OF PRECIPITATION AND TEMPERATURE

The profiles from the Tuştea and Bărbat valleys and location 6 on Sibişel show similar types of soil development. Field observations indicate that the depth to the calcic horizon was up to 40 cm; therefore, according to Retallack (2001), the mean annual rainfall did not exceed 600 mm. Moreover, calcretes associated with red soils form in climates with precipitation ranging from 100 to 500 mm per year (Khadkikar *et al*., 2000). The formation of smectite is also favoured by dry-wet climatic conditions (Chamley, 1989). The red coloration of the mudstone intercalations as well as the presence of these types of soils indicates a climate with wet-dry seasons and rainfall-evaporation interplay (Mack and James, 1994).

For Maastrichtian times, the temperature distribution map compiled by Chumakov *et al*. (1995) shows, for the Haţeg area situated at that time at latitude of 27±5°N, values of between 25 and 30°C. As today, the red calcisols already described are found in subtropical regions, temperatures between 25 and 30°C being too high for these types of palaeosol. Therefore we consider that temperatures between 20 and 25°C, in agreement with Amiot *et al*. (2004), are more realistic for that time. These temperatures were calculated for late Campanian-middle Maastrichtian latitudinal gradient, using the $\delta^{18}O$ record of phosphates from continental vertebrates.

The isotopic composition of the soil water in equilibrium with the calcite may be calculated using the measured oxygen isotopic compositions of calcretes and the inferred temperatures (Friedman and O`Neil, 1977). For Tuştea, the calculated values of soil water are between –5 (for 20°C) and –4‰ (for 25°C); for Pui, between –5.7 and –4.7‰ (SMOW). Using the linear relationship between soil carbonate and meteoric water deduced from actual pedogenic carbonate concretions (Cerling and Quade, 1993) the rain water in equilibrium with the carbonate concretions varied between –7 to –5‰ for both outcrops.

Regarding the eggshells, the empirical relationship between eggshell and drinking water composition (Sarkar and Bhattachary, 1991; Tandon *et al*., 1995; Johnson *et al*., 1998), indicates that the $\delta^{18}O$ of water which the species drunk was around –1‰ (SMOW). This indicates a 4 to 5‰ difference between the isotopic composition of precipitation calculated using the eggshell $\delta^{18}O$ and that calculated using the composition of palaeosol carbonates. Cojan *et al*. (2003) measured the isotopic composition of dinosaur eggshells and calcretes of Maastrichtian age from the Provence basin in France. They found a correlation between climate type and the difference in $\delta^{18}O$ (eggshell)– $\delta^{18}O$ (calcretes), and they concluded that strong evaporation favours a larger difference. We propose two different mechanisms in order to explain the isotopic distribution observed.

One possible explanation for the difference in $\delta^{18}O$ (eggshell)– $\delta^{18}O$ (calcretes) observed at Tuştea is the seasonal distribution of humidity, for which there is already strong evidence. At that time, Haţeg area was situated at a palaeolatitude of 27±5°N. Using the International Atomic Energy Agency/World Meteorological Organisation (IAEA/WMO,

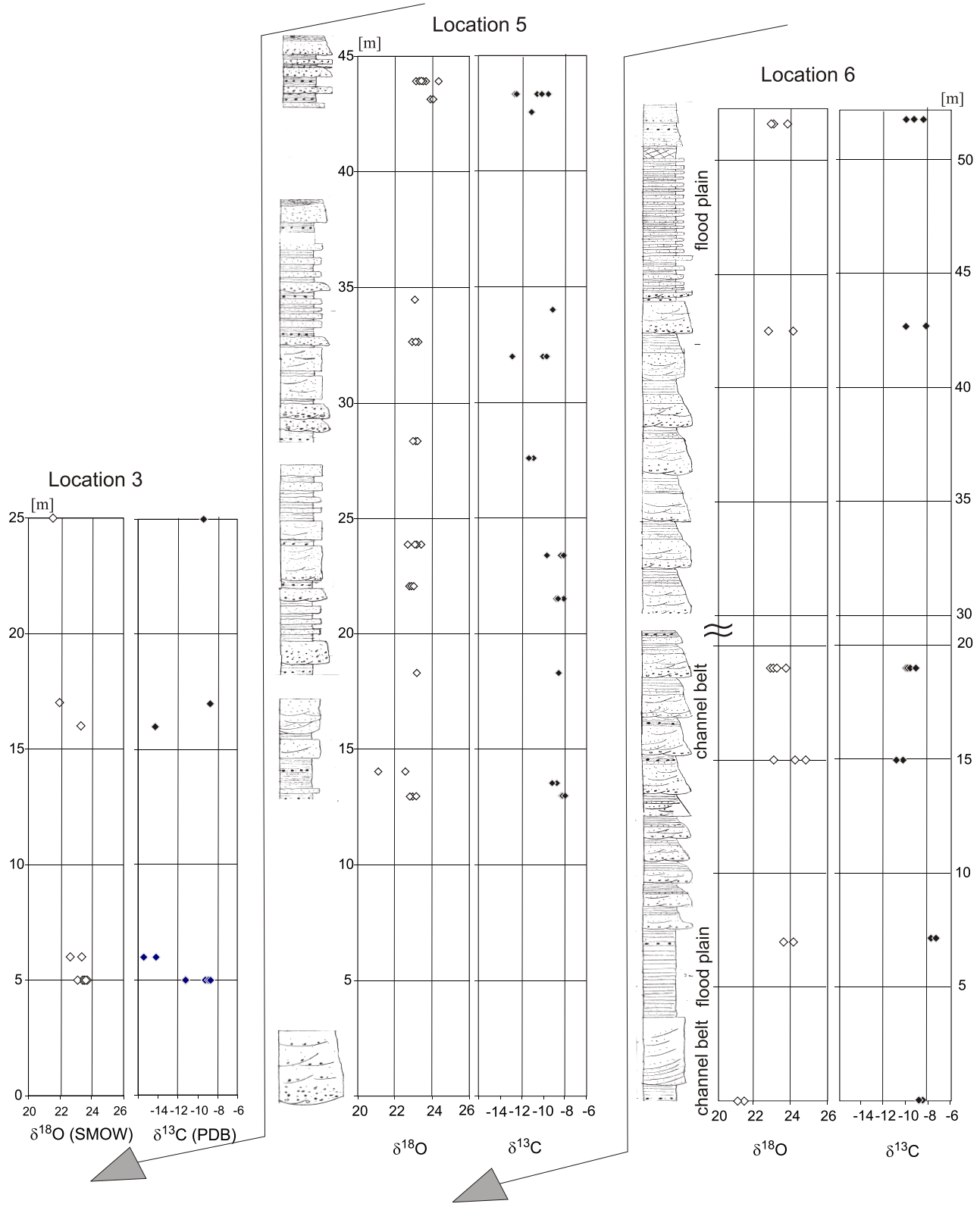

Fig. 8. Facies distribution and stable isotopic composition of calcretes along the Sibişel Valley

2001) database we compiled all the localities with precipitation between 100 and 800 mm/year, situated at latitudes between 25 and 35° north or south, and at elevations of less than 1000 m. For practically all stations, the seasonal $\delta^{18}O$ variation of rainwater is up to 5‰. The predominant pattern is one where a heavy $\delta^{18}O$ isotopic composition occurs during the dry, warm season (14 stations). Only for 6 stations, mostly related to monsoon-type climate, the amount effect is dominant over the temperature effect. During Maastrichtian times, the Haţeg basin was not situated in the vicinity of an open oceanic

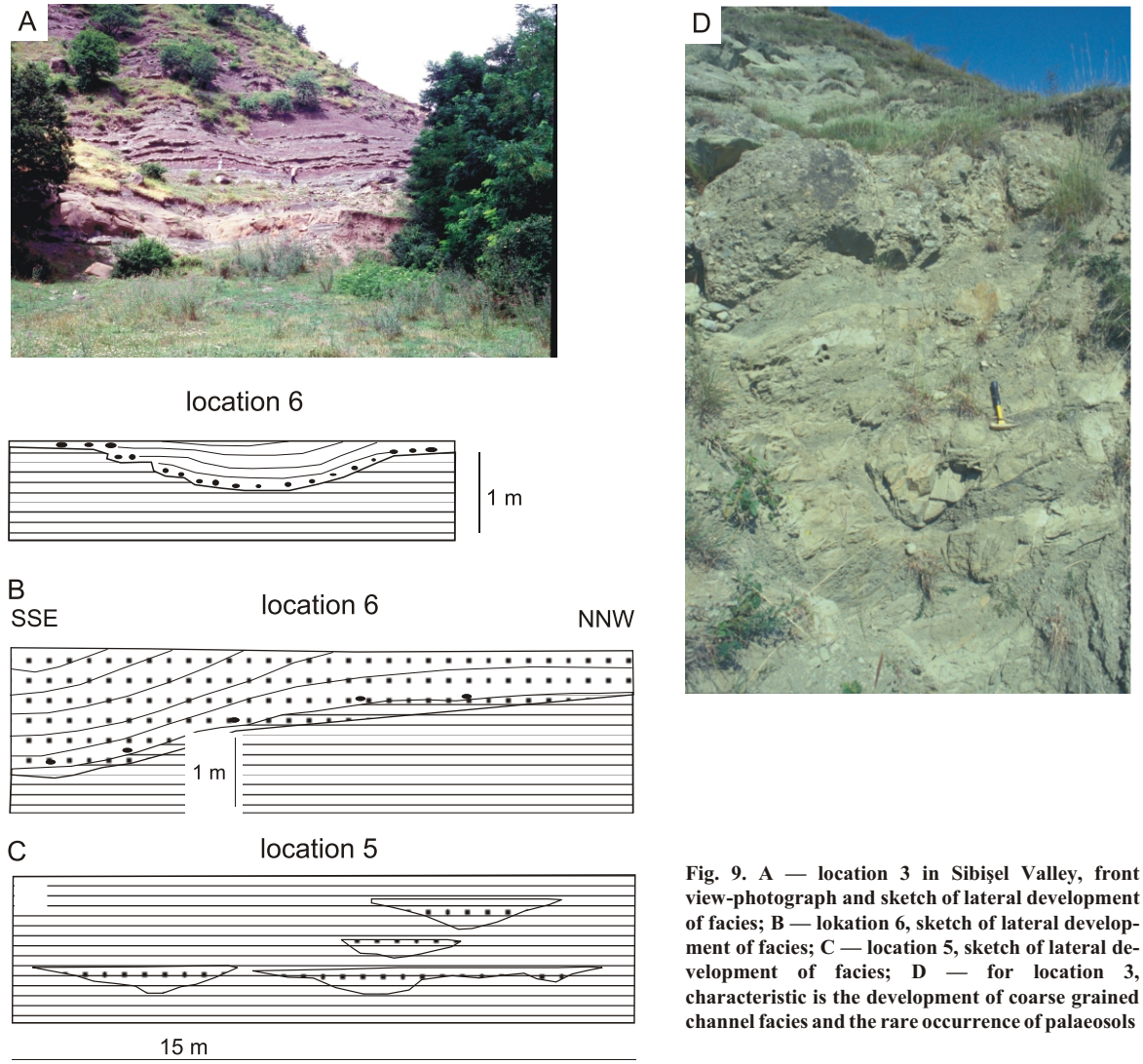

Fig. 9. A — location 3 in Sibişel Valley, front view-photograph and sketch of lateral development of facies; B — lokation 6, sketch of lateral development of facies; C — location 5, sketch of lateral development of facies; D — for location 3, characteristic is the development of coarse grained channel facies and the rare occurrence of palaeosols

domain but near to a land surrounded by sea, at a latitude of 27±5°C, so there is no support for strongly monsoon-dominated climatic conditions. Monsoon conditions also imply winds changing regularly in direction with minimal 120°, similar to winds which are present nowadays between 5° and 25° latitude (Goudie, 2002). Most likely the ^{18}O-enriched rain was related to the warm/(dry or wet) season. On a worldwide scale, the correlation between the isotopic composition of precipitation and temperature is well known (Dansgaard, 1964; Fricke and O`Neil, 1999) but the new IAEA data, together with palaeogeographical constraints concerning the position of the basin, make possible semi-quantitative estimations. We discuss further how seasonality could be related to the observed 4–5‰ differences between drinking water (calculated using the $\delta^{18}O$ of eggshells) and rain water (calculated using the $\delta^{18}O$ of calcretes). Dinosaurs needed some months to produce their eggs, but the time needed to eliminate the isotopic signature of the ingested water was much shorter. For example, modern birds need *ca*. 2 weeks to eliminate the isotopic signature of previously — ingested drinking water (Folinsbee *et al.*, 1970). Thus the heavier isotopic values calculated for drinking water could be explained by the fact that the eggs preserved the signature of the drinking water at the time they formed, and this was during the period characterized by heavier isotopic compositions of rainfall. Heavy $\delta^{18}O$ values of rain water were associated with warm, dry or wet, seasons. In contrast, carbonate concretions formed over a longer period of time, from 10 to 100 ky, thus reflecting a lower, long-term $\delta^{18}O$ average value of rain water.

Oxygen isotope compositions of eggshell carbonate are precipitated from dinosaur body waters. In comparison with the warm-blooded vertebrates, dinosaurs possess an additional variable — their body temperature. For vertebrates, the $\delta^{18}O$ value of body water is 4 to 8‰ higher than that of drinking water (Luz and Kolodny, 1985; D'Angela and Longinelli, 1993; Bryant and Froelich, 1995) for which we assume a similar composition as the rain water. The observed 4 to 5‰ enrichment observed between $\delta^{18}O$ (eggshell) and $\delta^{18}O$ (calcrete) could be due to the relative enrichment of $\delta^{18}O$ (body water) to $\delta^{18}O$ (drinking water) which is assumed to be similar to the composition of rain water.

In conclusion, both mechanisms, a dry season and enrichment of body water with respect to precipitation drive the oxygen isotopic composition of eggs to heavier values, and we cannot exclude an interplay of them.

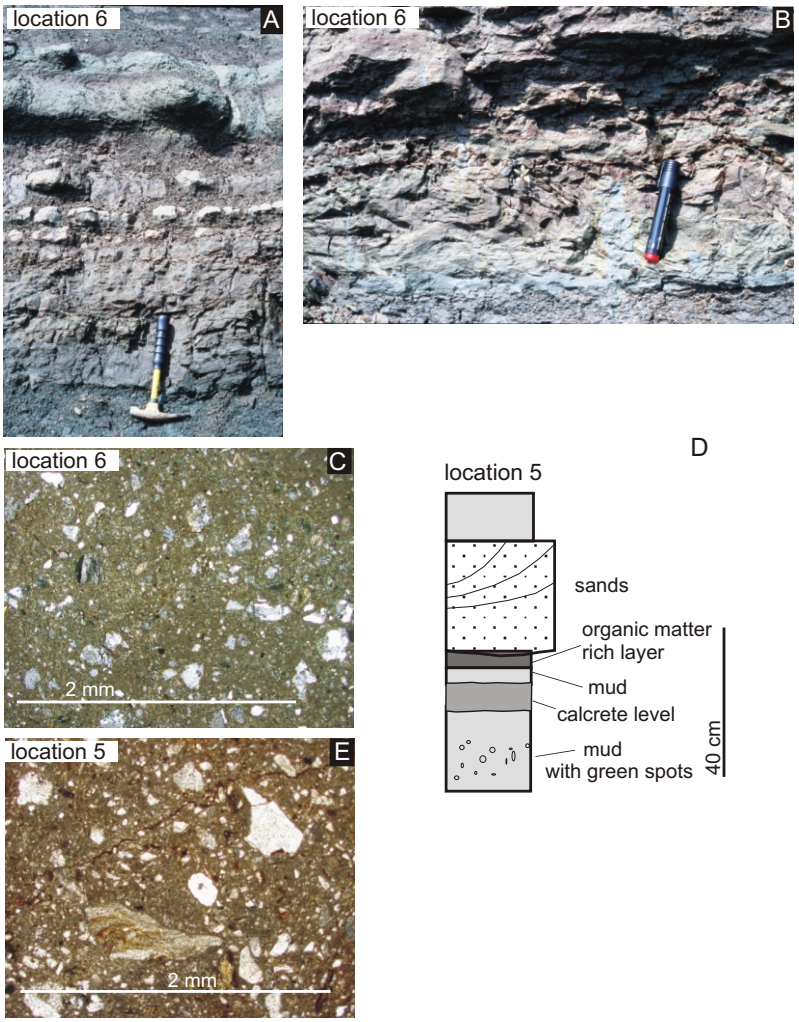

Fig. 10. A — palaeosol profile; B — swelling structure; C — thin section through a calcrete nodule; D — typical soil profile; E — micritic calcrete nodules

Along the Sibişel Valley, the shift by *ca*. 1‰ towards lower $\delta^{18}O$ values of carbonates may be related to several factors. For example, the progressive increase in the amount of annual rainfall will produce lighter precipitation; consequently the isotopic composition of concretions will become lighter. An increased amount of precipitation is also supported by the type of palaeosol, indicating higher humidity towards the upper part of the Sibişel section. Another explanation may be a trend to wards decreasing temperature, which has been documented for chron C31r of the Maastrichtian (Barrera, 1994; Barrera and Savin, 1999). This explanation was proposed also by Cojan *et al*., (2003) for a similar isotopic composition trend from in calcretes formed within palaeosols during chron C31 in the Provence basin, France. Both factors, increased amounts of precipitation and decreasing temperature, change the isotopic composition towards lower values, so that the negative isotopic excursion observed along the Sibişel Valley may reflect an interplay of them. As temperature controls hydrolysis, the trend towards lower temperatures is also supported by the change in composition of clay minerals from smectite-dominated (locations 6 and 5) to illite- and chlorite-dominated (location 3).

The presence of C3 versus C4 biomass (Park and Epstein, 1960; Bender, 1968), soil respiration rates and the CO_2 concentration in the air will control the carbon isotopic composition of carbonate concretions (Cerling, 1984; Quade *et al*., 1989). For the Tuştea and Bărbat valleys, the carbon isotopic compositions of calcretes vary between –8 and –6‰ and indicate a pure C3 ecosystem with a $\delta^{13}C$ isotopic composition of plants around –25‰. Along the Sibişel Valley, the values decrease from –8‰ at the bottom of the section (location 6) towards –12‰ at the top of the section (location 3). This may be due to a change in the type of vegetation, associated with more humid conditions. It is known that C3 plants growing under more humid conditions have lower C3 values than those growing on drier substrates. Fluctuations of the carbon isotopic composition of a few percent may be induced by this physiological effect (Farquhar *et al*., 1989).

For Tuştea, the measured $\delta^{13}C$ signatures of eggs range between –13 and –14‰. We also know that the eggs belong also

to a herbivorous dinosaur, *Telmatosaurus transsylvanicus*. Using the relation of Schaffner and Swart (1991), we have determined that the isotopic composition of the food source was around –29‰ (PDB). This value is similar but somewhat lighter than the isotopic composition of vegetation deduced from calcretes. This could be explained by the particular feeding habitats of this dinosaur and the preference for some plants rather than others.

Acknowledgements. Cristi and Cristina Panaiotu are thanked for discussions concerning palaeomagnetic data. F. Neubauer, C. Lecuyer and J. Van Itterbeek are thanked for constructive reviews. The manuscript benefited from their comments and corrections. We would like to acknowledge financial support from a MOEL Scholarship and FWF P16258.

REFERENCES

AMIOT R., LECUYER C., BUFFETTAUT E., FLUTEAU F., LEGENDRE S. and MARTINEAU F. (2004) — Latitudinal temperature gradient during the Cretaceous Upper Campanian-Middle Maastrichtian: $\delta^{18}O$ record of continental vertebrates. Earth Planet. Sc. Lett., **226**: 255–272.

ANASTASIU N. and CSOBUKA D. (1989) — Non-marine Uppermost Cretaceous deposits in Stei-Densuş region, (Haţeg basin): a sketch for a facial model. Rév. Roumaine Géol., Géophys., Géograph./Géol., 33–43–53.

ANTONESCU E., LUPU D. and LUP M. (1983) — Correlation palynologique du Cretace terminal du sud-est des Monts Metaliferi et de depression de Haţeg et de Rusca Montana. Ann. L´Inst. Geol. Geophys., Bucharest, **59**: 71–77.

ARTHUR M. A., DEAN W. E. and PRATT L. M. (1988) — Variations in the global carbon cycle during the Cretaceous related to climate, volcanism, and changes in atmospheric CO_2. In: The Carbon Cycle and Atmospheric CO_2: Natural Variations Archean to Present (eds. E. T. Sunquist and W. S. Broecker). Am. Geophys. Union.

BARRERA E. (1994) — Global environmental changes preceding the Cretaceous-Tertiary boundary: Early-Late Maastrichtian transition. Geology, **22**: 877–880.

BARRERA E. and SAVIN S. M. (1999) — Evolution of Late Campanian-Maastrichtian marine climates and oceans. In: Evolution of the Cretaceous Ocean-Climate System (eds. E. Barrera and C. C. Johnson). Geol. Soc. Am. Spec. Paper, **332**: 245–282.

BARRERA E., SAVIN S. M., THOMAS E. and JONES C. E. (1997) — Evidence for thermohaline-circulation reversals controlled by sea-level change in the latest Cretaceous. Geology, **25**: 715–718.

BARRON E. J. A. (1983) — A warm, equable Cretaceous: the nature of the problem. Earth Sc. Rev., **19**: 305–338

BARRON R. A. and WASHINGTON W. M. (1984) — The role of geographic variables in explaining paleoclimates: results from Cretaceous climate model sensitivity studies. J. Geophys. Res., **89**: 1267–1279.

BENDER M. M. (1968) — Variations in the $^{13}C/^{12}C$ ratios of plants in relation to the pathway of photosynthetic carbon fixation. Photochemistry, **10**: 1339–1344.

BERZA T., BALINTONI I., IANCU V., SEGHEDI A. and HANN H. P. (1994) — South Carpathians. Roman. J. Tecton. Region. Geol., **75**: 37–49.

BOJAR A.-V., GRIGORESCU D. and CSIKI Z. (2002) — Climatic record in Maastrichtian continental deposits of Southern Carpathians. Berichte des Institutes für Geologie und Paläontologie, Karl-Franzens Universität Graz, Band, **6**: 6–7.

BOJAR A.-V., GRIGORESCU D. and CSIKI Z. (2003) — Isotope analysis on mineral and biogenic carbonates from the Maastrichtian continental formations of the Haţeg Basin and their significance for the palaeoenvironment reconstruction. The 4th Romanian Symposium on Palaeontology, Cluj-Napoca, Abstract Volume: **10**.

BOJAR A.-V., NEUBAUER F. and FRITZ H. (1998) — Cretaceous to Cenozoic thermal evolution of the south-western South Carpathians: evidence from fission-track thermochronology. Tectonophysics, **297**: 229–249.

BRYANT J. D. and FROELICH P. N. (1995) — A model of oxygen isotope fractionation in body water of large mammals. Geochim. Cosmochim. Acta, **59**: 4523–4537.

BRINDLEY G. W. and BROWN G. (1980) — Crystal structures of clay minerals and their X-ray identification. Miner. Soc. London.

BUFFETAUT E., GRIGORESCU D. and CSIKI Z. (2002) — A new giant pterosaur with a robust skull from the Latest Cretaceous of Romania. Naturwissenschaften, **89**: 180–184.

CAMOIN G., BELLION Y., DERCOURT J., GUIRAUD R., LUCAS J., POISSON A., RICOU L-E. and VRIELYNCK B. (1993) — Late Maastrichtian (69.5 to 65 Ma). In: Atlas Tethys, Palaeonvironmental Maps (eds. J. Dercourt, L. E. Ricous and B. Vrielynck). Gauthier-Villars.

CANDE S. C. and KENT D. V. (1995) — Revised calibration of the geomagnetic polarity time scale for the Late Cretaceous and Cenozoic. J. Geophys. Res., **100** (B4): 6093–6095.

CERLING T. E. (1984) — The stable isotopic composition of modern soil carbonate and its relationship to climate. Earth Planet. Sc. Lett., **71**: 229–240.

CERLING T. and QUADE J. (1993) — Stable carbon and oxygen isotopes in soil carbonates. In: Climate Change in Continental Isotopic Records (eds. P. K. Swart, K. C. Lohmann, J. McKenzie and S. Savin). Geophys. Monogr., **78**: 217–231.

CHAMLEY H. (1989) — Clay Sedimentology. Springer Verlag.

CHUMAKOV N. M., ZHARKOV M. A., HERMAN A. B., DOLUDENKA M. P. *et al*. (1995) — Climatic zones in middle of the Cretaceous Period. Stratigraph. Geol. Correlat., **3**: 42–63.

CLARKE L. J. and JENKINS H. C. (1999) — New oxygen isotope evidence for long-term Cretaceous climatic changes in the Southern Hemisphere. Geology, **27** 699–702.

COJAN I., RENARD M. and EMMANUEL L. (2003) — Palaeonvironmental reconstruction of dinosaur nesting sites based on a geochemical approach to eggshells and associated palaeosols (Maastrichtian, Provence Basin, France). Palaeogeogr., Palaeoclimat., Palaeoecol., **191**: 111–138.

COLBERT E. H. (1973) — Continental drift and the distribution of fossil reptiles. In: Implications of Continental Drift to the Earth Sciences (eds. D. H. Tarling and S. K. Runcorn) 395–412.

CRAME J. A. (1992) — Review: Late Cretaceous paleoenvironments and biotas, an Antarctic perspective. Antarctic Sc., **4** 371–382.

CSIKI Z. and GRIGORESCU D. (1998) — Small theropods from the Late Cretaceous of the Haţeg Basin (Western Romania) — an unexpected diversity at the top of the food chain. Oryctos, **1**: 87–104.

CSIKI Z. and GRIGORESCU D. (2000) — Teeth of multituberculate mammals from the Late Cretaceous of Romania. Acta Paleont. Polon., **45** (1) 85–90.

D'ANGELA D. and LONGINELLI A. (1993) — Oxygen isotopes in living mammal's bones of Holocene age: palaeoclimatological considerations. Chem. Geol., **103**: 171–179.

DALLMEYER R. D., NEUBAUER F., FRITZ H. and MOCANU V. (1998) — Variscan vs. Alpine tectonothermal evolution of the South

Carpathian orogen: constraints from $^{40}Ar/^{39}Ar$ ages. Tectonophysics, **290**: 111–135.

DANIELS J. M. (2003) — Floodplain aggradation and pedogenesis in a semiarid environment. Geomorphology, **56**: 225–242.

DANSGAARD W. (1964) — Stable isotopes in precipitation. Tellus, **16**: 436–468.

DUCHAFOUR P. (1982) — Pedology. George Allen and Unwin, London.

FARQUHAR G. D., EHLERINGER J. R. and HUBICK K. T. (1989) — Carbon isotope discrimination and photosynthesis. Ann. Rev. Plant Phys. Plant Molecul. Biol., **40** 503–537.

FOLINSBEE R. E., FRITZ P., KROUSE H. R. and ROBBLEE A. R. (1970) — Carbon 13 and Oxygen 18 in dinosaur, crocodile and bird eggshells indicate environmental conditions. Science, **168**: 1353–1356.

FRAKES L. A. and FRANCIS J. E. (1990) — Cretaceous paleoclimates. In: Cretaceous Resources, Events and Rhythms (eds. R. N. Ginsburg and B. Beaudoin). NATO ASI, C, **304** 273–287.

FRAKES L. A., FRANCIS J. E. and SYKTUS J. I. (1992) — Climate modes of the Phanerozoic. Cambridge Univ. Press.

FRICKE H. C. and O`NEIL J. R. (1999) — The correlation between $^{18}O/^{16}O$ ratios of meteoric water and surface temperature: its use in investigating terrestrial climate change over geologic time. Earth Planet. Sc. Lett., **170**: 181–196.

FRIEDMAN I. and O`NEIL J. R. (1977) — Compilation of stable isotope fractionation factors of geochemical interest. In: Data of Geochemistry (ed. M. Fleischer). U.S. Geol. Surv. Prof. Pap. **440-KK**.

GOUDIE A. (2002) — Physische Geographie: eine Einführung. (4. Aufl.). Heidelberg.

GRIGORESCU D. (1983) — A stratigraphic, taphonomic and palaeoecologic approach to a "forgotten land": the dinosaur bearing deposits from the Haţeg Basin (Transylvania — Romania). Acta Palaeont. Polon., **28** (1–2): 103–121.

GRIGORESCU D. (1984) — New Theropod groups in the Maastrichtian of the Haţeg Basin: Coelurosaurians and Multituberculate Mammals, 3rd Symp. On Mesozoic Terrestrial Ecosystems, Attempto Verlag, Tübingen: 99–104.

GRIGORESCU D. (1993) — The latest Cretaceous dinosaur eggs and embryos from the Hateg Basin, Romania. Rev. Paleobiol., **7**: 95–99.

GRIGORESCU D., AVRAM E., POP G., LUPU M. and ANASTASIU N. (1990*a*) — Guide to excursions. International Symposium I.G.C.P. Projects 245: Nonmarine Cretaceous Correlation; Project, **282**: Tethyan Cretaceous Correlation, Bucharest.

GRIGORESCU D. and CSIKI Z. (2002) — Geological introduction to the Uppermost Cretaceous continental formations with dinosaurs and other vertebrates of the Haţeg Basin. In: The 7th European Workshop of Vertebrate Palaeontology, Abstract Vol. Excurs. Field Guide.

GRIGORESCU D. and HAHN G. (1987) — The first multituberculate teeth from the Upper Cretaceous of Europe (Romania). Geol. Palaeont., **21**: 237–243.

GRIGORESCU D., HARTENBERGER J.-L., RADULESCU C., SAMSON P. and SUDRE J. (1985) — Decouverte de mammiferes et dinosaures dans le Cretace superieure de Pui (Roumanie). Compt. Rend. l'Acad. Sc., Paris, Ser. II, **301**: 1365–1368.

GRIGORESCU D. and MELINTE M. (2001) — The stratigraphy of the Upper Cretaceous marine sediments from the NW Haţeg area (South Carpathians, Romania). Acta Palaeont. Rom., **3** 153–160.

GRIGORESCU D., SECLAMAN M., NORMAN D. B. and WEISHAMPEL D. B. (1990*b*) — Dinosaur eggs from Romania. Nature, 346, 417.

GRIGORESCU D., VENCZEL M., CSIKI Z. and LIMBEREA R. (1999) — New latest Cretaceous microvertebrate fossil assemblages from the Haţeg Basin (Romania). Geol. Mijnb., **98**: 310–314.

GRIGORESCU D., WEISHAMPEL D., NORMAN D. B, SECLAMAN M., RUSU M., BALTRES A. and TEODORESCU V. (1994) — Late Maastrichtian dinosaur eggs from the Haţeg Basin (Romania). In: Dinosaur Eggs and Babies (eds. K. Carpenter, K. F. Hirsch and J. R. Horner): 75–87. Cambridge Univ. Press.

GRÜNFELDER M., POPESCU G., SOROIU M., ARSENESCU V. and BERZA T. (1983) — K-Ar and U-Pb dating of the metamorphic formations and the associated igneous bodies of the Central South Carpahtians. Ann. Instit. Geol. Geofiz., **61**: 37–46.

HUBER B. T. and WATKINS D. K. (1992) — Biogeography of Campanian-Maastichtian calcareous plankton in the region of the southern ocean: paleogeographic and paleoclimatic implications. In: The Atarctic Paleoenvironment: a Perspective on Global Change (eds. J. P. Kennett and D. A. Warnke) 31–60. Am. Geophys. Union.

HUBER B. T., NORRIS R. D. and MACLEOD K. G. (2002) — Deep-sea paleotemperature record of extreme warmth during the Cretaceous. Geology, **30** 123–126.

IAEA/WMO (2001) — Global Network of Isotopes in Precipitation. The GNIP Database. Accessible at: www.isohis.iaea.org.

JOHNSON B. J., FOGEL M. L. and MILLER G. H. (1998) — Stable isotopes in modern ostrich eggshell: a calibration for paleoenvironmental applications in semi-arid region of southern Africa. Geoch. Cosmochim. Acta, **62**: 2451–2461.

KAUFFMAN E. G. (1973) — Cretaceous bivalvia. In: Atlas of Paleobiogeography (ed. A. Hallam) 353–383. Elsevier.

KHADKIKAR A. S., MERH S. S., MALIK J. N., CHAMYAL L. S. (2000) — The character and genesis of calcrete in Late Quaternary alluvial deposits, Gujarat, western India, and its bearing on the interpretation of ancient climates. Palaeogeogr., Palaeoclimat., Palaeoecol., **162**: 239–261.

KINTER E. B. and DIAMOND S. (1956) — A new method for preparation and treatment of oriented aggregate samples of soil clays for X-ray diffraction analysis. Soil Sc., **81**: 111–120.

KRÄUTNER H. G. (1996) — Alpine and Pre-Alpine terranes in the Romanian South Carpathians and equivalents south of the Danube. In: Terranes of Serbia (eds. V. Knezevic and B. Krstic): 53–58.

KRUMBEIN W. E. and GARRELS R. M. (1952) — Origin and classification of chemical sediments in terms of PH and oxidation-reduction potential. J. Geol., **60**: 1–33.

KUYPERS M. M. M., PANCOST R. D. and DAMSTE J. S. S. (1999) — A large and abrupt fall in atmospheric CO_2 concentration during Cretaceous times. Nature, **399**: 342–345

LI L. and KELLER G. (1998) — Abrupt deep-sea warming at the end of the Cretaceous. Geology, **26** 995–998.

LLOYD C. R. (1982) — The Mid-Cretaceous earth: paleogeography, ocean circulation, temperature and atmospheric circulation. J. Geol., **90** 393–413.

LUZ B. and KOLODNY Y. (1985) — Oxigen isotope variations in phosphate of biogenic apatites, IV. Mammal teeth and bones. Earth Planet. Sc. Lett., **75**: 29–36.

MACK G. H. and JAMES C. W. (1994) — Palaeoclimate and the global distribution of palaeosols. J. Geol., **102**: 360–366.

MJOS R., WALDERHAUG O. and PRESTHOLM E. (1993) — Crevasse splay sandstone geometries in the Middle Jurassic Ravenscar Group of Yorkshire, U.K. In: Alluvial Sedimentation (eds. M. Marzo and C. Puigddefabregas). Spec. Publ. Int. Ass. Sediment., **17**: 167–184.

MOORE D. M. and REYNOLDS R. C. Jr. (1997) — X-ray diffraction and the identification and analysis of clay minerals. Oxford Univ. Press, New York.

NEUBAUER F. (2002) — Contrasting Late Cretaceous to Neogene ore provinces in the Alpine-Balkan-Carpathian-Dinaride collision belt. In: The Timing and Location of Major ore Deposits in an Evolving Orogen (eds. D. J. Blundell, F. Neubauer and A. Quadt). Geol. Soc. (London) Spec. Pub., **204**: 81–102.

NOPCSA F. VON (1902) — Über das Vorkommen der Dinosaurier bei Szentpéterfalva. Zeitschrift der Deutschen Geologischen Gesellschaft, **1902** 34–39.

NOPCSA F. Von (1900) — Dinosaurierreste aus Siebenbürgen. Schädel von Limnosaurustransylvanicus nov. Gen. Et spec. Denkschriftern der kaiserlichen Akademie der Wissenschaften Wien, Mathematisch-naturwissenschaftliche Classe, **68**: 555–591.

NOPCSA F. Von (1914) — Die Lebensbedingungen der obercretacischen Dinosaurier Siebenbürgens. Centralblatt für Mineralogie, Geol. Paläont., **1914**: 564–574.

NOPCSA F. Von (1915) — Erdély dinoszauruszai. Magyar királyi Földtani Intézet Évkönyve, **23** (1): 3–24.

NOPCSA F. Von (1923) — On the geological importance of the primitive reptilian fauna in the Uppermost Cretaceous of Hungary; with the description of a new tortoise. Quarter. J. Geol. Soc. London, **74**: 100–116.

NOPCSA F. Von (1926) — Osteologia reptilium fossilium et recentium. Fossilium Catalogus. I Animalia, **27** 1–391.

OLIVERO E. B., GASPARINI Z., RINALDI C. A. and SCASSO R. (1991) — First record of dinosaurs in Antarctica (Upper Cretaceous, James Ross Island): paleogeographic implications. In: Geological Evolution of Antarctica (eds. M. R. A. Thomson, J. A. Crame and J. W. Thompson) 617–622. Cambridge Univ. Press.

PANA I., GRIGORESCU D., CSIKI Z. and COSTEA C. (2002) — Palaeo-ecological significance of the continental gastropod assemblages from the Maastrichtian dinosaur beds of the Hateg Basin. Acta Palaeont. Roman., **3** 337–343.

PANAIOTU C. (1998) — Palaeomagnetic constraints on the geodynamic history of Romania. In: Monograph of Southern Carpathians (ed. J. Sledzinski). Report. Geodes., **7**: 205–216.

PANAIOTU C. and PANAIOTU C. (2002) — Palaeomagnetic studies. In: The 7th European Workshop of Vertebrate Palaeontology. Abstract Vol. Excurs. Field Guide: **59**.

PARK R. and EPSTEIN S. (1960) — Carbon isotope fractionation during photosynthesis. Geochim. Cosmochim. Acta, **21**: 110–126.

PĂTRAŞCU ST., BLEAHU M., PANAIOTU C. and PANAIOTU C. E. (1992) — Palaeomagnetic study of the Upper Cretaceous magmatic rocks from the western part of South Carpathians (Romania): tectonic implications. Tectonophysics, **213**: 341–352.

QUADE J., CERLING T. E. and BOWMAN J. R. (1989) — Systematic variations in the carbon and oxygen isotopic composition of pedogenic carbonate along elevation transects in the southern great Basin, United States. Geol. Soc. Am. Bull., **101**: 464–475.

RADULESCU C. and SAMSON P.-M. (1986) — Precisions sur les affinities des Multitubercules (Mammalia) du Cretace superieur de Romanie. C. R. Acad. Sc. Paris, **2** (304): 1825–1830.

RETALLACK G. J. (1991) — Miocene Paleosols and Ape Habitats of Pakistan and Kenya. Oxford Univ. Press, New York.

RETALLACK G. J. (1998) — Fossil soils and completeness of the rock and fossil record. In: The Adequacy of the Fossil Record (eds. S. K. Donovan and C. R. C. Paul): 131–162.

RETALLACK G. J. (2001) — Soils of the past. An introduction to palaeopedology. Blackwell Sc.

RIEDMÜLLER G. (1978) — Neoformations and transformations of clay minerals in tectonic shear zones. TMPM Tschermak. Mineral. Petrograph. Mitteilun. **25**: 219–242.

RUDDIMAN W. F. and PRELL W. L. (1997) — Introduction to the uplift, Climate Connection. In: Tectonic Uplift and Climate Change (ed. W. F. Ruddiman) 3–15. Plenum Press, New-York and London.

SANDULESCU M. (1984) — Geotectonica Romaniei. Editura Tehnica, Bucuresti.

SARKAR A. and BHATTACHARY S. K. (1991) — Stable-isotope analyses of dinosaur eggshells: palaeoenvironmental implications. Geology, **19**: 1068–1071.

SCHAFFNER F. C. and SWART P. K. (1991) — Influence of diet and environmental water on the carbon and oxygen isotopic signatures of seabird eggshell carbonate. Bull. Marine Sc., **48**: 23–38.

SCHULTZ L. G. (1964) — Quantitative interpretation of mineralogical composition from x-ray and chemical data of the Pierre Shales. Geol. Surv. Proff. Paper, **391C**: 1–31.

SMITH T., CODREA V. A., SASARAN E., VAN ITTERBEECK J., BULTYNCK P., CSIKI Z., DICA P., FARCAS C., GARCIA G. and GODEFROIT P. (2002) — A new exceptional vertebrate site from the Late Cretaceous of Haţeg Basin (Romania). Studia Univ. Babes-Bolyai, Geol., Spec., **1**: 321–330.

STANISTREET I. G. and McCARTHY T. S. (1993) — The Okavango fan and the classification of subaerial systems. Sediment. Geol., **85**: 115–133.

STILLA A. (1985) — Geologie de la region de Haţeg-Cioclovina-Pui-Banita (Carpathes meridionales). An. Instit. Geol. Geofiz., **66**: 92–197.

TANDON S. K., SOOD A., ANDREWS J. E. and DENNIS P. F. (1995) — Palaeoenvironments of the dinosaur-bearing Lameta Beds (Maastrichtian), Narmada Valley, Central India. Palaeogeogr., Palaeoclimat., Palaeoecol., **117**: 153–184.

THOREZ J. (1975) — Phyllosilicates and clay minerals. Lelotte, Dison.

TRIBUTH H. (1991) — Notwendigkeit und Vorteil der Aufbereitung von Boden- und Lagerstättentonen. In: dentifizierung und Chg von Tonminerale (eds. H. Tributh and G. Lagaly). In, Berichte der DTTG, **1**: 29–33.

VAKHRAMEEV V. A. (1991) — Jurassic and Cretaceous floras and climates of the earth. Cambridge Univ. Press.

Van ITTERBEECK J., SASARAN E., CODREA V., SASARAN L. and BULTNYCK P. (2004) — Sedimentology of the Upper Cretaceous mammal-and dinosaur-bearing sites along the Râul Mare and Bărbat rivers, Haţeg basin, Romania. Cretaceous Res., **25**: 517–530.

WEISHAMPEL D. B., JIANU C.-M., CSIKI Z. and NORMAN D. B. (2003) — Osteology and phylogeny of Zalmoxes, an unusual eurnithopod dinosaur from the latest Cretaceous of Romania. J. Systemat. Palaeont. 65–123

WEISHAMPEL D. B., NORMAN D. B. and GRIGORESCU D. (1993) — Telmatosaurus transsylvanicus from the Late Cretaceous of Romania: the most basal hadrosaurid dinosaur. Palaeontology, **36**: 361–385.

WHITTIG L. D. (1965) — X-ray diffraction techniques for mineral identification and mineralogical composition. In: Methods of Soil Analysis. (ed. C. A. Black). Am. Soc. Agronomy, **1**: 671–698.

WILLINGSHOFER E. (2000) — Extension in collisional orogenic belts: the Late Cretaceous evolution of the Alps and Carpathians, Ph.D. thesis, Amsterdam.

WILLINGSHOFER E., ANDRIESSEN P., CLOETHING S. and NEUBAUER F. (2001) — Detrital fission track thermochronology of Upper Cretaceous syn-orogenic sediments in the South Carpathians (Romania): inferences on the tectonic evolution of a collisional hinterland. Basin Res., **13**: 379–395.

WILSON M. J. (1989) — A handbook of determinative methods in clay mineralogy. Verlag Blackie Verlag.